VACUUM AND ELECTRON CLOUD ISSUES AT THE GSI PRESENT AND FUTURE FACILITIES

G. Rumolo*, O. Boine-Frankenheim, E. Mustafin, I. Hofmann,
GSI, Darmstadt, D-64291, Germany

Abstract

According to the international accelerator project at GSI, the double synchrotron SIS100/300 and a chain of storage rings will be built (using the present GSI synchrotron SIS18 as injector) in order to achieve high intensity and high energy heavy ion pulses for nuclear or plasma physics studies or anti-proton production. Dynamic vacuum instability and electron cloud are potential intensity limiting factors in the SIS18 and SIS100/300, which need to be investigated. Dynamic vacuum instability induced by ion loss due to charge exchange presently limits the intensity in the SIS18 to a few 10^9 U^{28+}, well below the design goal value needed for the future facility. NEG-coating of the vacuum chamber surface and a system of collimators to intercept the beam losses in a controlled way are the measures presently under study to push up the instability threshold. A broad simulation campaign aimed at defining possible electron cloud issues in the SIS18 and in the SIS100/300 shows on the other hand that the thresholds for electron cloud build up in terms of SEY are rather high. Parameters like SEY and dimensions of the beam vacuum chamber for SIS100/300 have been swept over wide ranges of values, and good sets for the safe ring operation are thus identified.

INTRODUCTION

With strong participation from its users and the international science community, GSI has developed over the past few years definite plans to expand its present facility into a major new international accelerator facility, which will use the existing GSI system as an injector [1]. Following an evaluation advisory committee to the German federal government, and its recommendation to construct the facility, in 2003 the government has approved the construction under condition that 25% of the total cost be covered by international partners.

The central goals for the new facility are essentially to increase the intensity of the ion beams, their energy, and to provide secondary beams with unprecedented features: intense beams of short-lived nuclei up to 1–2 GeV/u, high quality and energy antiproton beams, both with the option of storage and cooling, and for in-ring experimentation.

The intensity of "low energy" ion beams, i.e. beams around 1–2 GeV/u, is expected to go up by about two orders of magnitude over the actual present performance. This will be achieved by increasing the cycling rate of the injector, the existing synchrotron SIS18, by a factor 5. A second factor ten is expected to be gained from reducing the charge state of the Uranium beam from +73 to +28. The most important consequence of this will be the increase in secondary beam intensities, i.e. beams of short-lived nuclei ("radioactive beams"), by three or four orders of magnitude. This comes from the fact that, in addition to the primary beam intensity increase, collection efficiency and storage of secondary beams will be optimized. Ion beams of high charge state and thus higher energy, up to 30-35 GeV/u for medium to heavy masses, will also become available at substantially increased intensities over the present facilities.

The SIS18 needs to be upgraded to inject about 2.5×10^{11} U^{28+} beams into the new SIS100 with a repetition frequency of 4 Hz. The SIS100 will therefore be able to accelerate, rebucket and deliver 10^{12} U^{28+} beams with a frequency of 1 Hz. 2.5×10^{11} U^{28+} ions in the SIS18 actually represents a value very close to the space charge limit of this machine. Unfortunately, the present situation shows that a yet lower bound exists, coming from a pressure run away initiated by ion loss due to stripping in the residual gas. The vacuum instability and the current study of counter-measures and solutions is described in detail in Sect. II. Besides, the experience of other proton/ion machines operating with bunched beams has proven the potential danger of formation of electron clouds in the beam chamber [2]. Causing vacuum degradation, additional heat load (to be avoided in rings with superconducting dipoles, as SIS100 is planned to be) and possibly beam instabilities, these might limit the machine performance in the range of parameters in which it is supposed to operate. This consideration has motivated the electron cloud study presented in Sects. III and IV, for SIS18 and SIS100, respectively.

U^{28+} LIFETIME MEASUREMENTS AT THE GSI-SIS18

A theoretical study to describe the vacuum instability induced by the lost particles in heavy ion accelerators is applied to the U^{28+} beam lifetime measurements in the SIS18 at GSI, where pressure run away is presently one of the main concerns for high-intensity operation. The desorption yield at the injection energy of 11.4 MeV/u is extrapolated from these measurements and compared to the values obtained in the GSI test stand and in other laboratories..

Model

In order to study the pressure evolution inside the vacuum chamber of an accelerator taking into account the out-

* G.Rumolo@gsi.de

gassing induced by the beam, we use the equation [3]:

$$\frac{\mathrm{d}P}{\mathrm{d}t} = -\frac{1}{\tau_\mathrm{p}}(P - P_e) + \frac{N\beta\mathrm{c}P}{V}\left(\eta_\mathrm{ion}\sigma_\mathrm{ion} + \eta_\mathrm{loss}\sigma_\mathrm{loss}\right) \quad (1)$$

where P_e is the static pressure (without beam) in the chamber, τ_p is the pumping time equal to the ratio between the chamber volume V and the effective pumping speed S_ef, N is the total number of ions in the machine, $\beta\mathrm{c}$ the ion velocity, σ_ion and σ_loss are the target and projectile ionization cross sections, η_ion and η_loss are the desorption yields for gas ions repelled to the walls or ions lost from the beam, respectively. The pressure P in Eq. (1) is the total pressure averaged along the ring:

$$P(t) = \int_0^L P(x,t)xdx \quad (2)$$

The condition for vacuum instability can be easily derived from Eq. (1):

$$(\eta_\mathrm{ion}\sigma_\mathrm{ion} + \eta_\mathrm{loss}\sigma_\mathrm{loss})N < \frac{S_\mathrm{ef}}{\beta\mathrm{c}} \quad . \quad (3)$$

If we neglect that the recoil momentum from Rutherford scattering can accelerate the ionized rest gas molecules to energies that can be as high as few MeV (this issue is actually still under study, but the above assumption might be reasonably justified if the cross section of this process is very low with respect to that of other processes), the desorption due to gas ions hitting the wall is normally much lower than that induced by the high energy lost ions. Eq. (3) writes then more conveniently:

$$N < N_\mathrm{thr} = \frac{S_\mathrm{ef}}{\beta\mathrm{c}\eta_\mathrm{loss}\sigma_\mathrm{loss}} \quad . \quad (4)$$

The number of particles N that appears in Eqs. (1), (3) and (4) is not a constant and its evolution is given by the equation of lifetime:

$$\frac{\mathrm{d}}{\mathrm{d}t}\left(\ln\frac{N}{N_\mathrm{i}}\right) = -\sigma_\mathrm{L}\beta\mathrm{c}\frac{P}{k_\mathrm{B}T} \quad , \quad (5)$$

where k_B is the Boltzmann constant, T the temperature, and N_i the initial number of particles in the accelerator. Equations (1) and (5) represent a set of coupled equations, which need to be solved together to allow an accurate prediction of pressure evolution and particle loss in a certain machine operation [4]

Threshold of vacuum instability in the SIS18

Figures 1 and 2 show a clear evidence of a pressure run away in the SIS18 affecting U^{28+} beams with $N_\mathrm{i} = 1.4 \times 10^9$ and 5.3×10^9. This suggests that we are in both cases above the instability threshold dictated by Eq. (4).

A set of 4 measurements, including the two shown in the pictures, has been used to extrapolate linear pumping speed S_ef, loss cross section σ_loss,desorption coefficient η and static pressure P_e. Results of this analysis are resumed in Table I [5].

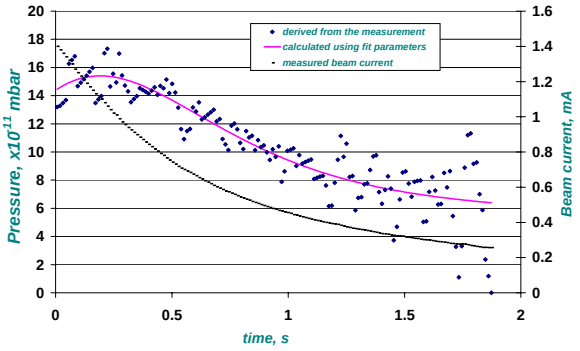

Figure 1: Measured beam current of U^{28+} ions circulating at a constant energy $E = 8.9$ MeV/u in the SIS18 and corresponding fit of pressure evolution. Injected current $I_0 = 1.4$ mA

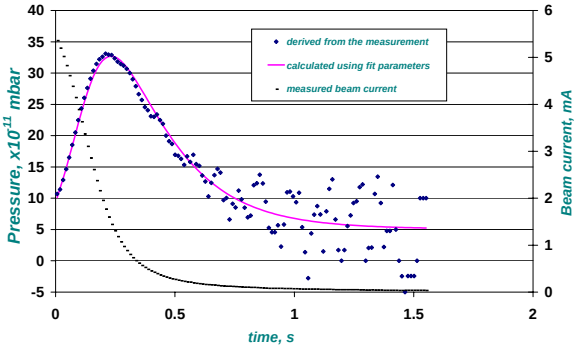

Figure 2: Measured beam current of U^{28+} ions circulating at a constant energy $E = 8.9$ MeV/u in the SIS18 and corresponding fit of pressure evolution. Injected current $I_0 = 5.3$ mA

With the data derived from the fit, the stability condition (4) sets the limit on the maximum number of particles which can be injected into the SIS18 to $\approx 10^9$ ions in a single pulse.

To cure the vacuum instability an increase of pumping speed and a decrease of desorption yield would be a direct solution. Installation of NEG-coated stripes into the vacuum chamber can increase the local pumping speed up to about 2000 l s^{-1} m^{-1} [6]. NEG coating of one SIS18 superperiod (the one containing the injection section, which

Table 1: SIS18 parameters as inferred from the fit of lifetime measurements.

N_i (10^9)	s_ef (l/s/m)	σ (Mbarn)	η	p_e (mbar)
1.08	89	110	20000	6×10^{-11}
1.4	67	80	27000	14×10^{-11}
1.97	89	130	16000	6.5×10^{-11}
5.36	82	210	11000	10×10^{-11}

seems to be the most troublesome due to the high injection losses) is planned for the next machine shut down. A special treatment of the vacuum chamber surface, or use of special materials can decrease the effective desorption yield. In order to investigate the viability of this solution a test-stand experiment is currently used at GSI (see next subsection). Also, specially designed collimators placed downstream from the dipoles to intercept and cut the stray ions could help to keep the pressure bumps under control [7]. Pumps should then be installed in proximity of the collimator to pump the desorbed gas away: the amount of this desorbed gas can be reduced by causing the ions to hit perpendicularly on the collimator. The main drawback of this solution is the tight design of these collimators, which in order to be effective should be transversely put at about 2σ from the axis. An efficient collimator design has been presently developed for the new ring SIS100 (whose lattice has been optimized to ease the charge separation between main beam and different charge state ions), but the problem still remains under study for the already existing SIS18. There finally exists the possibility to replace the U^{28+} beam with a higher charge state beam (U^{73+}), since the capture dominated projectile ionization cross section for U^{73+} is lower than the stripping cross section for U^{28+}. Besides, the capture cross section (since for high charge states capture is the dominant process) quickly decreases with energy [8], so that the situation becomes even less critical during and after the ramp. The shortcoming of this solution lies in that higher charge states allow injecting lower numbers of ions into the ring due to the space charge limit scaling like Z^{-2}. The limit for U^{73+} is for example 4×10^{10} against the 2.5×10^{11} U^{28+}, which we could in principle inject into the SIS18 if there were no vacuum limitations.

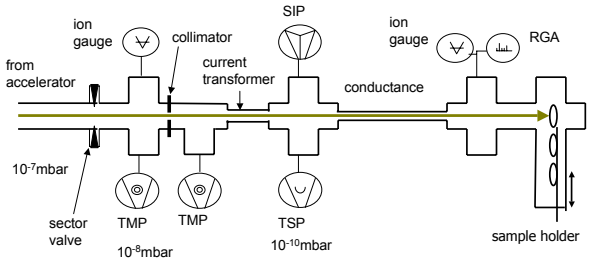

Figure 3: Experimental set up to measure the ion induced desorption yield

Desorption yield measurements at the GSI test stand

A new experimental test-stand has been set up at GSI to measure the ion induced desorption yield. The idea is to get more detailed information on the mechanism of desorption. The dependence of the yield on the charge state, energy and mass of the incident ion is under investigation. Also different kinds of beam pipe material (stainless steel, copper, ceramics) and different types of surface treatments and coatings are being examined.

A schematical view of the experimental setup is shown in Fig. 3. The ion beam is coming from the left. and reaches the measurement chamber through a conductance. The measurement chamber is equipped with a beam screen, an ion gauge and a residual gas analyser (RGA). The desorption yield is found from the detected pressure increase in the measurement chamber after the ion beam hits the target. Some results for different sorts of ions on different target materials are shown in Fig. 4. The values obtained, lower by one order of magnitude with respect to those extrapolate from the U^{28+} lifetime measurements in the SIS18, are explainable with the lower energy of the projectile ions and their normal incidence.

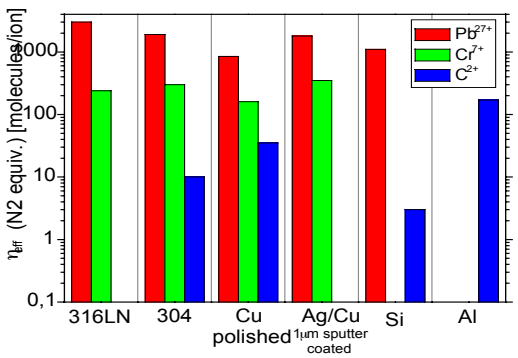

Figure 4: Measured desorption yields for different sorts of projectile ions (energy $E = 1.4$ MeV/u) on different target surfaces for perpendicular incidence

ELECTRON CLOUD IN THE SIS18

The experience of a number of machines around the world has shown that electron clouds are presently associated with the main limitations in the performance of positively charged particle accelerators [2].

The SIS18 upgrade (to deliver the currents that need to be injected into the planned SIS100/300 synchrotrons) is expected to bring the existing ring into a high intensity regime substantially never explored before. All the essential parameters to be reached are summarized in Table 2.

Two high current scenarios (4×10^{10} U^{73+} ions inside the machine) are presently taken into consideration, consisting in a 4-bunch or single bunch scheme. In the 4-bunch scheme, each bunch would have a parabolic longitudinal profile and would carry 10^{10} ions over a fairly long extension (≈ 20 m). Alternatively, the single bunch would be a very long quasi-coasting beam inside a barrier bucket (full length about 150 m). Both scenarios have been simulated with the ECLOUD code [9].

Figures 5 and 6 show the expected electron cloud build up in field-free region with the 4 bunches and the one long bunch, respectively, circulating in the SIS18. We observe an exponential growth of the number of electrons when

Table 2: SIS18 parameters used for the simulations.

C	216 m
N_{b}	4×10^{10} U^{73+}
E_{kin}	1 GeV/u
Num. bunches	1 or 4
Long. bunch shape	Parabolic or uniform
Transverse bunch shape	Gaussian
σ_{z}	5 m, 37.5 m
σ_{p}/p_0	1.06×10^{-3}
α	0.0356
$\epsilon_{\mathrm{x,yN}}$	$6.5/5$ μm
$Q_{\mathrm{x,y,s}}$	$4.308/3.29/1.4\times10^{-3}$
$\xi_{\mathrm{x,y}}$	corrected or -1
δ_{max}	scanned from 1.8 to 2.2
$h_{\mathrm{x,y}}$	$10, 5$ cm
P_{e}	0.1 nTorr
σ_{ion}	2 MBarn/u

the secondary emission yield is above 2.1 in the first case, whereas the one long bunch appears to be stable against electron multipacting up to quite high maximum SEYs of the chamber wall (maximum simulated δ_{max} is 2.3). From picture 5, it becomes clear that for $\delta_{\mathrm{max}} \leq 2.0$ no significant electron accumulation occurs inside the ring. However, values of δ_{max} greater than 2.0 cause an electron cloud to be formed, whose saturation density values stay in the range $1.5 - 3.5 \times 10^{11}$ m^{-3} when $\delta_{\mathrm{max}} < 2.3$, but can definitely grow to values higher than 10^{12} m^{-3} for larger maximum SEY's. The rule according to which the electron cloud saturates at line density values that approximately equal the beam line density, which has been found to be true for many machines slightly beyond the threshold of electron cloud onset [10], appears to be violated in the SIS18. This is probably due to the different regime of multipacting that we find in the SIS18 with respect to most positron or proton machines operating with short bunches (such as the SPS with the LHC-type beam or the KEK Low Energy Ring). In the SIS18 the electrons oscillate many times within one bunch passage, which suggests that the multiplication comes from a combined effect of trailing edge acceleration and survival of electrons between bunches due to the elastic reflection. This process is illustrated in Fig. 7, which shows the bunch structure and the relative electron generation for the 4-bunch case. Most electrons are secondaries produced during the falling phase of the bunch, but the electron cloud formation is only made possible by a bunch-to-bunch accumulation effect.

We can easily evaluate the number of oscillations performed by one electron during one bunch passage by using the formula [11]:

$$n_{\mathrm{ex(y)}} = \frac{1}{\pi}\sqrt{\frac{Z N_{\mathrm{b}} l_{\mathrm{b}} r_{\mathrm{e}}}{2\sigma_{\mathrm{x(y)}}(\sigma_{\mathrm{x}} + \sigma_{\mathrm{y}})}} \qquad (6)$$

For the SIS18, the above formula yields $n_{\mathrm{ex,y}} = 11.2$ when 4 bunches are inside the machine, and $n_{\mathrm{ex,y}} = 61.3$ for the long bunch case. In the latter case, the absence of electron cloud is probably also helped by the 10 m rising and falling edges of the barrier bucket, which can certainly limit the trailing edge multiplication.

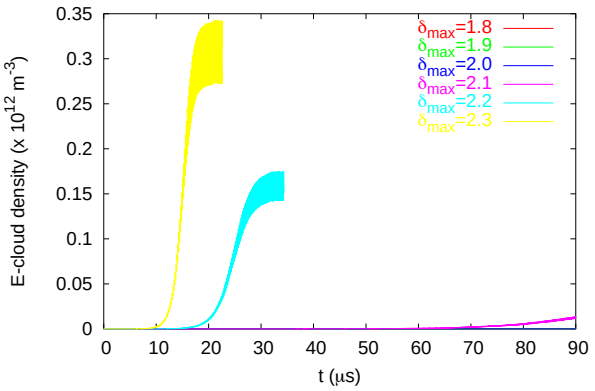

Figure 5: Electron cloud build up for 4 bunches in the SIS18 and different maximum SEY's (field-free region).

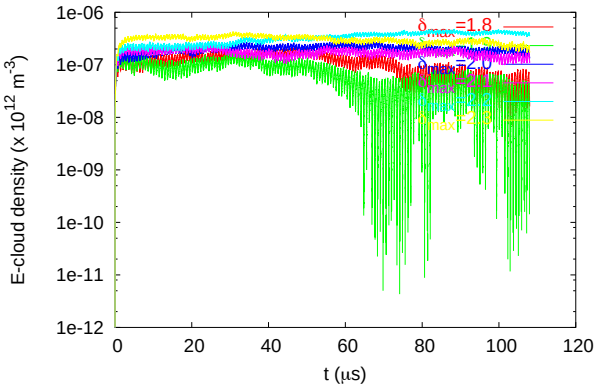

Figure 6: Electron accumulation for one long bunch in the SIS18 and different maximum SEY's. There is no electron cloud formation for maximum SEY's up to 2.3.

Simulations of electron cloud build up in a strong dipole region show that the situation becomes more critical in the presence of a strong magnetic field. Fig. 8 clearly shows that the threshold decreases to $\delta_{\mathrm{max}} = 1.9$ and the cloud forms much more rapidly than in field-free space. Saturation values of the cloud density do not differ much from those obtained in the field-free case, and they still range between $1 - 3 \times 10^{11}$ m^{-3}. The cloud is in this case mainly concentrated in the central part of the beam pipe, since we have assumed that primary electrons come from beam induced gas ionization, and they multipact along vertical lines being thereabout confined by the strong magnetic field lines.

An instability study has been carried out for some of the cases when an electron cloud is expected to build up

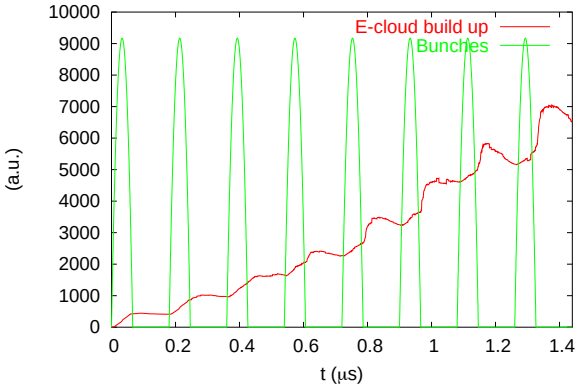

Figure 7: 4 bunches in the SIS18: bunch structure and start-up of the electron accumulation. Trailing edge and bunch-to-bunch effects are both clearly visible in the cloud dynamics.

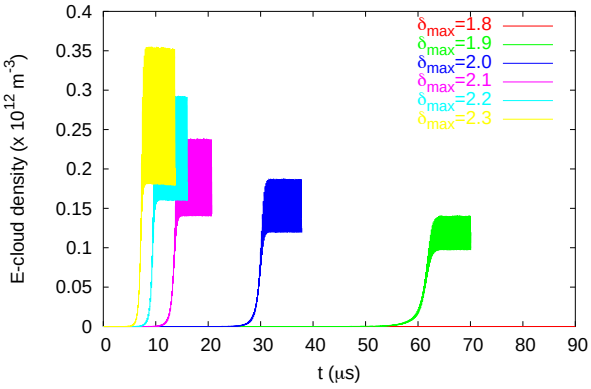

Figure 8: Electron cloud build up for 4 bunches in the SIS18 and different maximum SEY's (strong dipole).

in the SIS18. The values of the cloud density have been inferred from the build up simulations discussed above, and actually scanned over a range of plausible numbers.

In particular, we have used the HEADTAIL code [12] to simulate the single bunch instability of a bunch interacting with the electron cloud in the 4-bunch scheme. In some cases the beam becomes unstable exhibiting both coherent dipole motion and emittance growth. Figures 9 and 10 show examples of vertical centroid motion for cloud densities $\rho_e = 1 - 3 \times 10^{11}$ m^{-3}. In these simulations, both horizontal and vertical chromaticities were set to zero. In reality, the SIS18 operates without chromaticity correction, and therefore chromaticities can be close to their natural values, which is about -1 in units of $\xi = (\Delta Q/Q_0)/(\Delta p/p_0)$. While such a high value of $\xi_{x,y}$ can damp the coherent dipole motion, it does not seem to affect the emittance growth. This can be probably explained by observing that the emittance growth takes place over a time scale which is significantly shorter than the synchrotron period (strong head-tail coupling [13]), and therefore chromaticity cannot affect it much (contrary to the regular head-tail coupling).

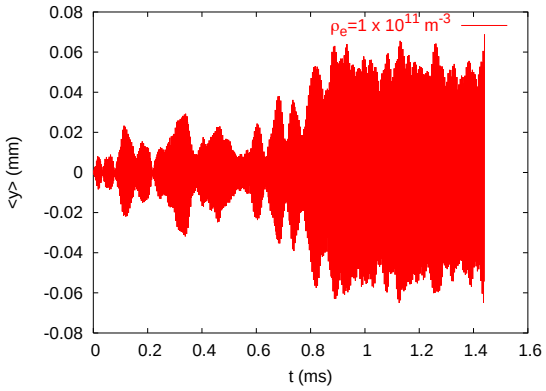

Figure 9: Vertical dipole motion of a bunch in the SIS18 for the 4-bunch scheme and an electron cloud density of $10^{11} m^{-3}$.

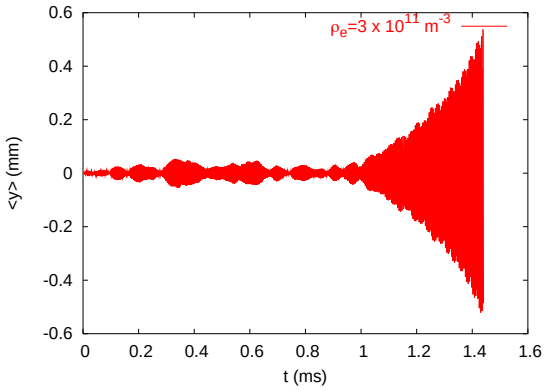

Figure 10: Vertical dipole motion of a bunch in the SIS18 for the 4-bunch scheme and an electron cloud density of 3×10^{11} m^{-3}.

ELECTRON CLOUD STUDY FOR SIS100

A typical set of parameters for the operation of SIS100 is shown in Table 3. 10^{12} U^{28+} are injected from the SIS18 and then delivered downstream for further use with 1 Hz repetition rate. These ions are packed in 8 bunches, leaving two empty buckets since the rf system of SIS100 will work with harmonic number $h = 10$. The 240 ns bunch spacing seems quite high compared to that of machines exhibiting evidence of electron cloud, and could therefore be enough to prevent electron cloud formation at the planned beam intensities. To study the build up we have simulated different maximum SEY's as well as different chamber sizes and shapes. The Cimino-Collins parametrization of the SEY has been used [14], assuming therefore that the electrons have probability 1 to be elastically reflected if they impinge on the beam pipe with vanishing energy. The chamber sizes have been swept in the range 6–12 cm, and circular as well as elliptical flat shapes have been considered. The primary

source of electrons has been assumed to be either the residual gas ionization or electron desorption from ion losses. The electron desorption rate for lost ions has been assumed 100-1000, whereas the losses have been optimistically set to 2% s^{-1}. These numbers bring about an electron production rate from losses that can be up to 2–3 orders of magnitude higher than that from residual gas ionization alone.

Table 3: SIS100 parameters used for the simulations.

C	1080 m
N_b	10^{12} U^{28+}
E_{kin}	2.7 GeV/u
Num. bunches	8
Long. bunch shape	Parabolic
Transverse bunch shape	Gaussian
Bunch spacing	240 ns
σ_z	9 m
$\sigma_{x,y}$	1.0/1.0 cm
δ_{max}	scanned from 1.8 to 2.2
$h_{x,y}$	6 to 12 cm
P_e	3.8×10^{-3} nTorr
σ_{ion}	2 MBarn/u

Figure 11 shows that elliptical flat chambers can inhibit the cloud build up even for maximum SEY's as high as 2.2. As the chamber shape gets more round, the threshold decreases and finally sits between 1.9 and 2.0 for round chambers with a radius of 12 cm. In all cases, maximum SEY's up to 1.8 seem to allow a safe operation of SIS100.

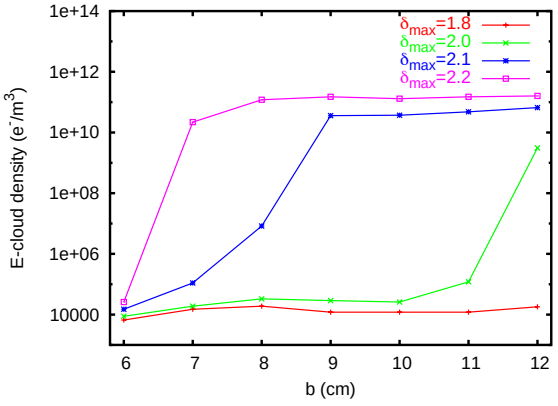

Figure 11: Electron cloud density values at saturation for different chamber vertical sizes and different maximum SEY's (field-free region).

Figure 12 shows that in presence of a dipole field, the electron cloud forms even for chamber sizes that do not cause electron cloud in field-free region.

To compare the two different mechanisms of primary electron generation, we can observe in Fig. 13 how the density of electrons in the beam chamber is much higher

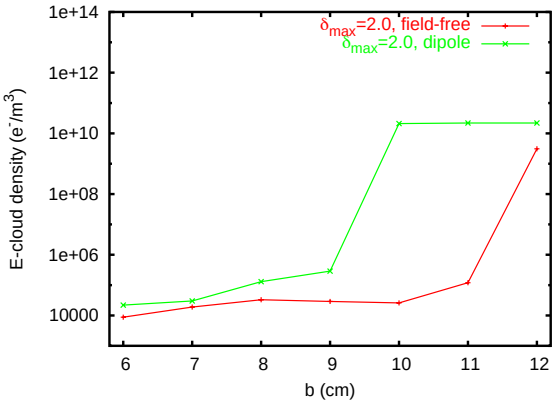

Figure 12: Electron cloud density values at saturation for different chamber vertical sizes and field-free or dipole regions (maximum SEY fixed to 2.0).

when the electrons are generated via ion losses than via gas ionization. Nevertheless, the density at saturation is the same when the machine operates in multipacting regime, demonstrating thus that, if a multiplication process is indeed present, the primary source of electrons is not essential. In this case, electrons accumulate up to a saturation density value which in only determined by the balance between repulsive space charge from the electrons themselves and the secondary emission process. Figure 14 shows how electrons accumulated through multipacting grow to the same saturation density value independently whether the seed electrons were from residual gas ionization or from ion losses. Only the rise time of the cloud is much shorter in the latter case due to the much higher number of primaries.

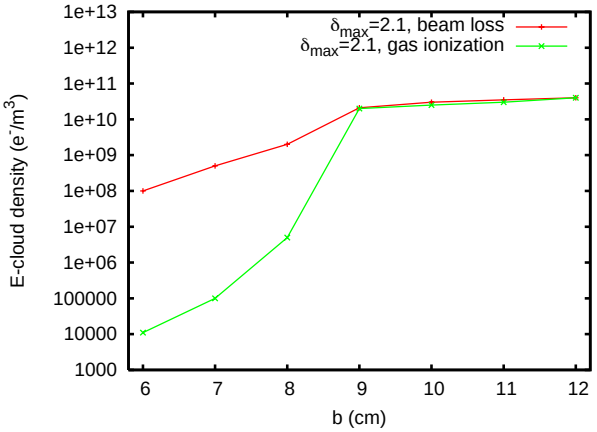

Figure 13: Electron cloud density values at saturation for different chamber vertical sizes and different seed electrons, from rest gas ionization or ion loss induced desorption (maximum SEY fixed to 2.1).

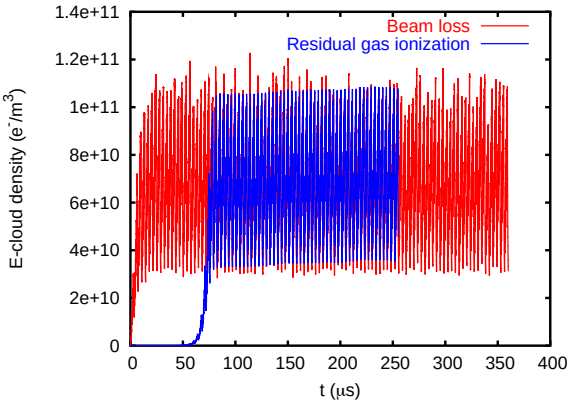

Figure 14: Electron cloud build up for a maximum SEY of 2.1 and different mechanisms of primary electron production.

CONCLUSIONS

To serve as an injector for the new synchrotron SIS100, the existing synchrotron SIS18 needs to upgraded to accelerate and deliver 2.5×10^{11} U^{28+} ions with a 4 Hz repetition rate. The present limit to the SIS18 performance comes from a severe vacuum instability that sets in when the number of particles in the ring exceeds a few 10^9, causing a pressure run away and rapid beam loss. The reason of this instability seems by now to have been identified in strong desorption from the pipe walls induced by lost ions hitting the walls at grazing angles. A number of countermeasures are currently under study to circumvent this problem and raise the threshold of the vacuum instability. These mainly consist in a more efficient pumping through NEG coating and/or a system of collimators to localize and control the beam losses. Another possibility would be to use higher charge state Uranium ions (73+), which have the advantage of a lower capture cross section. The drawback of this choice would be that the number of particles eventually injected into the SIS100 would decrease by almost a factor 10 due to the lower space charge limit.

If vacuum still seems to be a serious issue for the GSI International Accelerator Project, the electron cloud, on the other hand, is not expected to be of any concern for the future operation because of its high build up threshold. Maximum SEY's below 1.8 seem to be safe both for the SIS18 in upgraded operation and for the SIS100. Such values can be easily achieved with proper surface treatment of the inner pipe walls in both rings.

ACKNOWLEDGMENTS

The authors would like to thank A. Krämer, H. .Kollmus, H. Reich-Sprenger, M. Bender, E. Mahner, P. Spiller, F. Zimmermann, G. Bellodi, R. Cimino, and many others for providing information and for numerous helpful discussions.

REFERENCES

[1] An International Accelerator Facility for Beams of Ions and Antiprotons; Conceptual Design Report 11/2001; http://www.gsi.de/GSI-Future/cdr/

[2] H. Fukuma, K. Cornelis, F.-J. Decker, R. Macek, E. Métral, W. Fischer in Proceedings of ECLOUD'02, CERN, Geneva 15-18 April 2002, edited by G. Rumolo and F. Zimmermann, Yellow Report CERN-2002-001

[3] A. G. Mathewson, "Vacuum System Design", in: S. Turner (Ed.) Proceedings of CAS "Fifth General Physics Course", Vol. II, CERN 94-01, 1994, p. 717

[4] O. Boine-Frankenheim and G. Rumolo, "Beam life time calculations for SIS18 and SIS100", to appear as GSI Internal Report.

[5] E. Mustafin *et al.*, Nucl. Inst. Methods A **510** (2003) 199-205

[6] E. Mahner, "Technical Design of the LEIR Vacuum System", LHC-VAC/EM Technical Note 2002-04

[7] C. Omet and P. Spiller, GSI-Acc-Note-2004-03-001

[8] A. S. Schlachter, *et al.*, Phys. Rev. **A 30**, 722 (1984).

[9] G. Rumolo and F. Zimmermann, "Practical User Guide for ECLOUD" CERN-SL-Note-2002-016 (AP), 2002

[10] F. Zimmermann, "Electron Cloud Simulations: an Update" in Proceedings of the LHC Workshop Chamonix XI, CERN SL-2001-003 DI

[11] G. Rumolo, and F. Zimmermann "Theory and Simulation of the Electron Cloud Instability" in Proceedings of the LHC Workshop Chamonix XI, CERN SL-2001-003 DI

[12] G. Rumolo and F. Zimmermann, "Practical User Guide for HEADTAIL" CERN-SL-Note-2002-036 (AP), 2002

[13] A. W. Chao, *Physics of Collective Beam Instabilities in High Energy Accelerators*, John Wiley & Sons, Inc. (1993)

[14] R. Cimino, I. R. Collins, M. A. Furman, M. Pivi, F. Ruggiero, G. Rumolo, and F. Zimmermann "Can low energy electrons affect high energy physics accelerators ?" Phys. Rev. Letters **93** 014801 (2004)